Supporting Information

Composite thin film of simultaneously formed carbon and SnO_2 QDs for supercapacitance application

*Aarti P. Gaikwad, Sagar H. Patil, Kashinath R. Patil, Shivaram D. Sathaye and Chandrashekhar V. Rode**

A. P. Gaikwad, Dr. S. H. Patil, Dr. C. V. Rode

CSIR-National Chemical Laboratory,

Dr. Homi Bhabha Road, Pashan, Pune- 411008, India.

Email: cv.rode@ncl.res.in

Tel. No. : 91-020 25902349

Mob. No. : 9423531022.

Dr. S. D. Sathaye

759/83 Deccan Gymkhana,

Pune-411004, India.

Dr. K. R. Patil

39, Yoganand Park I, Paud Road,

Kothrud, Pune-411038, India.

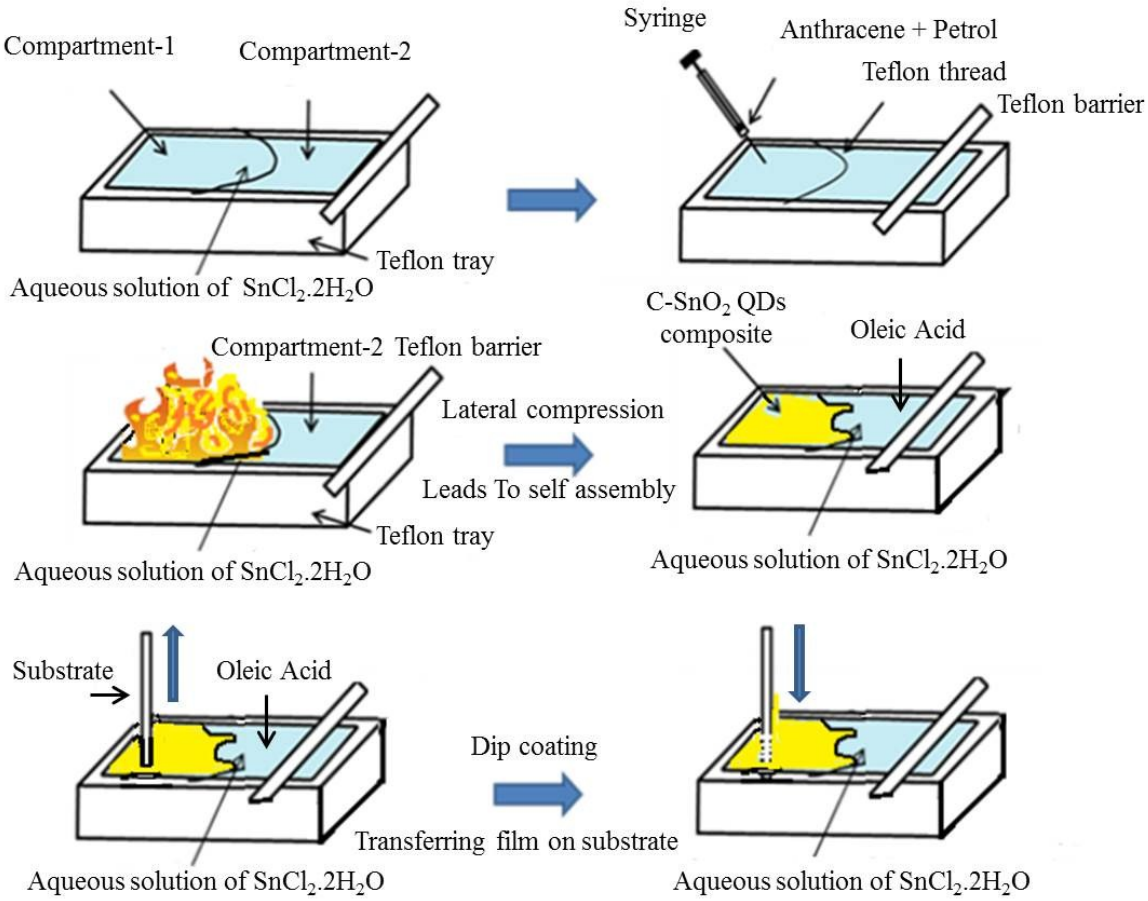

Scheme S1 Schematic illustration of synthesis of C-SnO_2 composite thin film

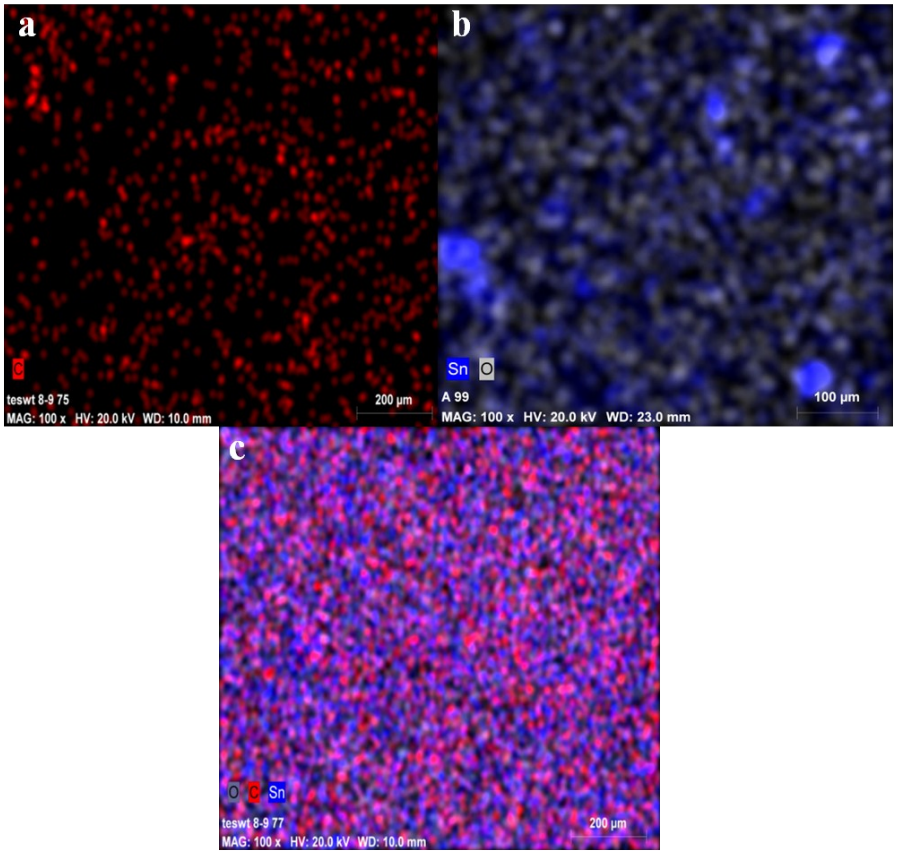

Figure S1 Elemental mapping of C QDs (a), SnO_2 (b) and C-SnO_2 QDs composite (c) respectively.

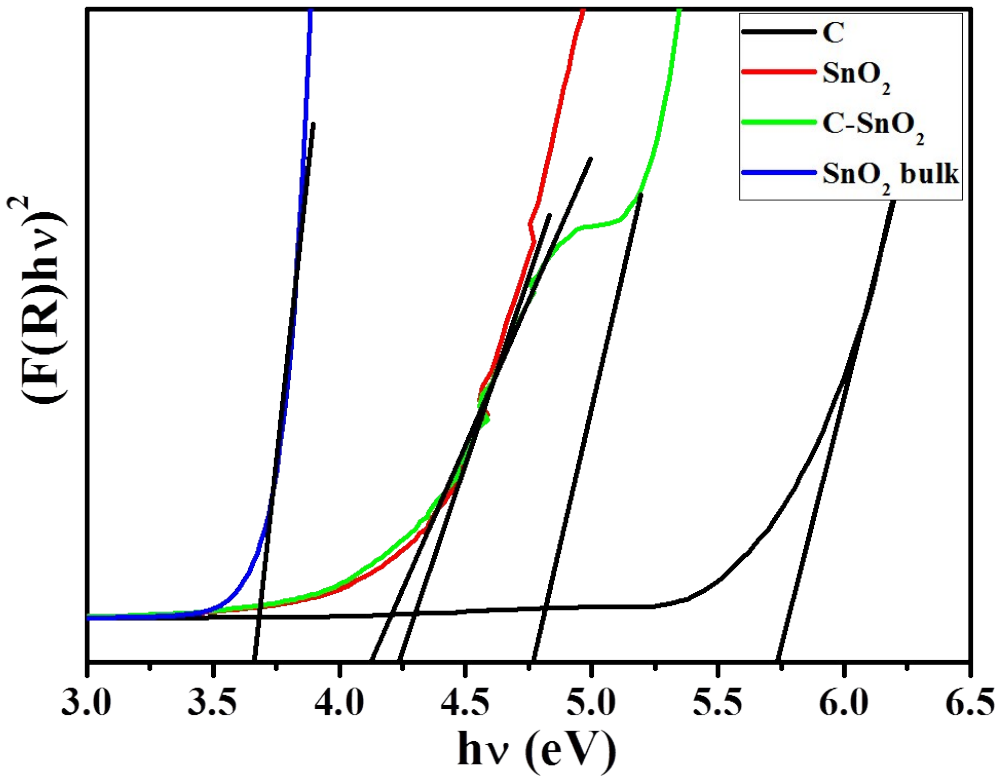

Figure S2: Tauc plots of C, SnO_2, C-SnO_2 QDs and SnO_2 bulk using diffuse reflectance data Kubelka- Munk function (KM).

UV-visible absorption spectroscopy is a powerful technique to explore the optical properties of semiconducting nanocrystalline thin films. Bohr radius of SnO_2 is 2.7 nm. Particle sizes smaller than the Bohr radius (QDs), lead to quantum confinement effects. The band gap of bulk crystalline SnO_2 is reported to be 3.6 eV. In the present case, a clear, although broad, absorption peak is shown at 225 nm for SnO_2 QDs and 270-300 nm for C-SnO_2 composite QDs film respectively. The absorption in nanomaterials in general and QDs in particular occurs by excitonic transition in HOMO-LUMO gap as against electronic transition from valance to conduction band in case of crystalline solids. Excitonic transition at room temperature is a typical feature observed in nano-material semiconductors, especially, QDs due to quantum confinement effect.

The energy gap of semiconducting materials can be calculated by extrapolation of the tangent to Tauc's plots based on the equation:

$$[F(R)h\upsilon]^{1/n} \alpha \quad h\upsilon - E_g$$

Where F(R) is modified Kubelka–Munk function,

$$F(R) = \frac{(1-R)^2}{2R}$$

R is reflectance measured from the DRS of samples and n = ½ for direct band gap of material while n = 2 for indirect band gap of material.

From Tauc's plot the blue shift of absorption edge is clearly observed as compared to their bulk counterparts, which clearly demonstrate the quantum confinement effect of the nanoparticles. The estimated band gap from the Tauc plot of the C, SnO_2, C-SnO_2 QDs composite and SnO_2 bulk are about 5.7, 4.24, 4.14, 4.75, and 3.67 eV respectively. It was not surprising that we observe two absorption band edges for composite, which is similar to the observation of Umarao et al. [S1] for TiO_2 and Gr composite.

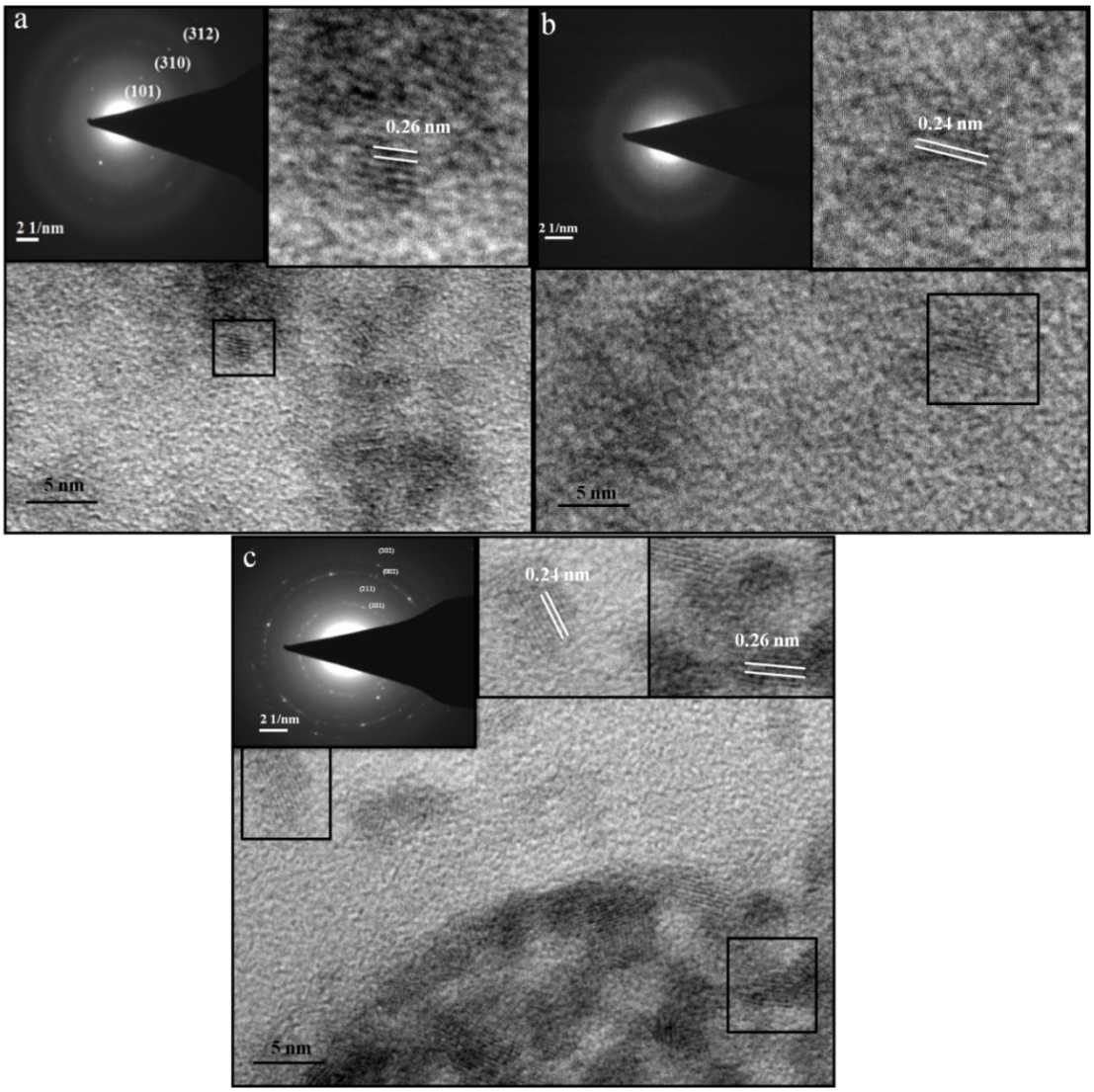

Figure S3 HRTEM image of SnO_2 (a), C QDs (b), and C-SnO_2 (c); right insect is enlarge image of marked square and left insect is SAED image of the sample respectively.

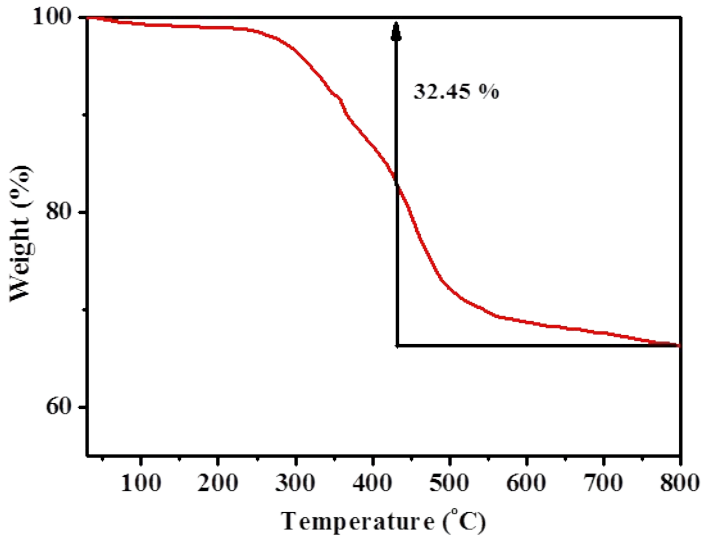

Figure S4 TGA of the C-SnO_2 composite.

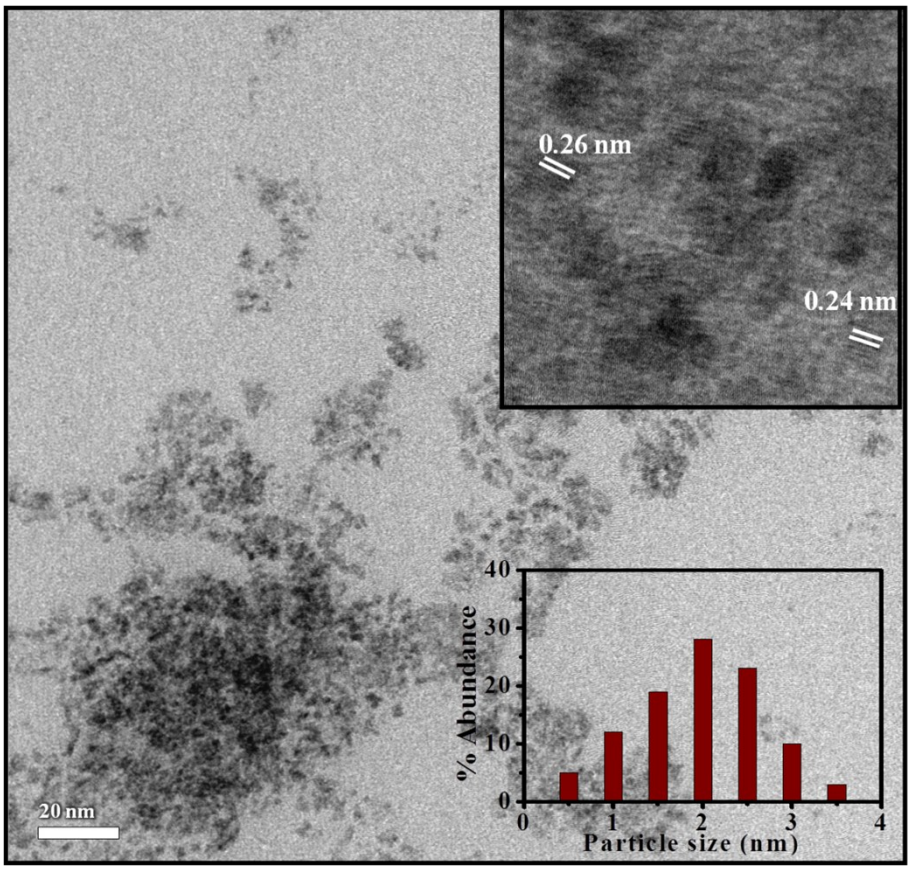

Figure S5 TEM image of the C-SnO_2 composite after electrochemical performance and the insets is particle size histogram (bottom right), HRTEM image (top right) respectively.

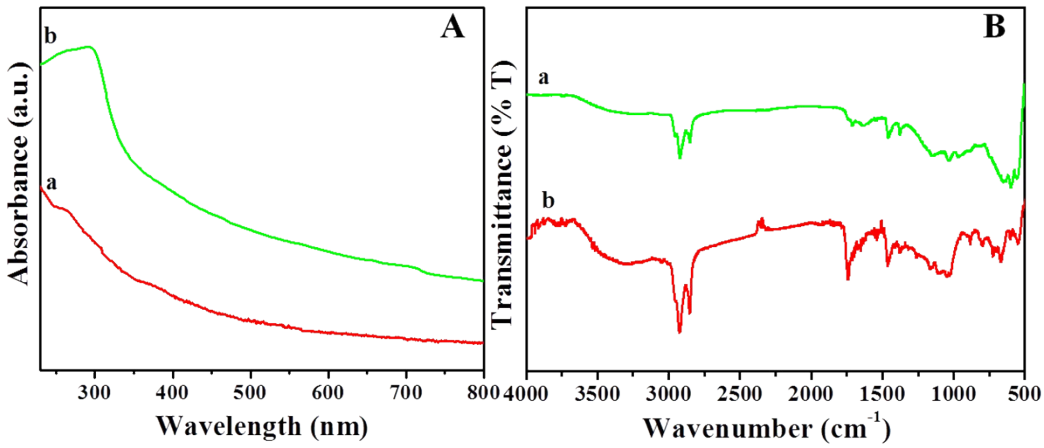

Figure S6 UV-Visible spectra (A), FTIR spectra (B) of C-SnO_2 composites before (a) after (b) 1000th charge/discharge cycles, respectively.

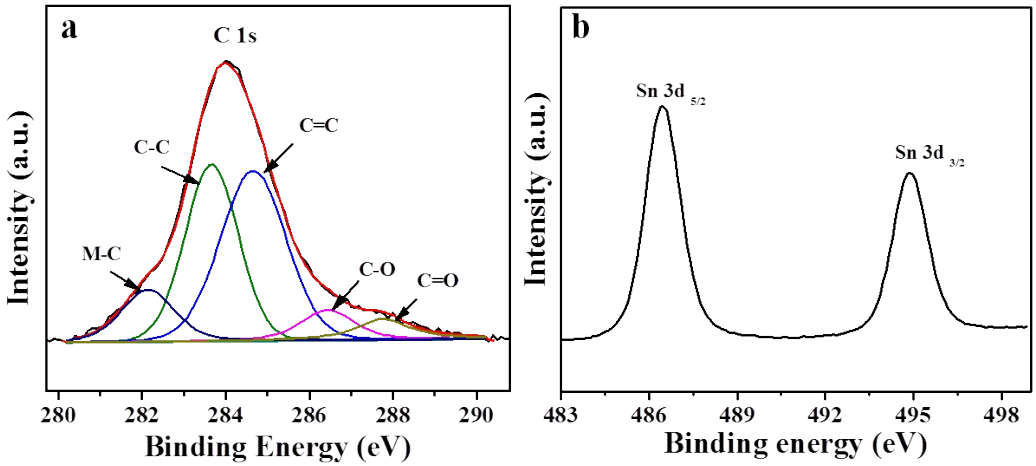

Figure S7 XPS spectra (a) deconvoluted C 1s and (b) Sn 3d of C-SnO_2 composites respectively after 1000th charge/discharge cycles.

The deconvoluted C 1s spectrum of C-SnO_2 composite after charging/discharging cycle gives 5 peaks. The binding energy 282.1, 283.6, 284.7, 286.5 and 287.8 corresponds to metal-carbon, C-C sp^3, C=C sp^2 and C-OH and -COOH groups respectively. Moreover, the high resolution XPS spectra for Sn in composite (**Figure S7** (b)) shows two distinct peaks at 486.4 and 494.9 eV attributed to Sn $3d_{5/2}$ and Sn $3d_{3/2,}$ respectively assignable to Sn +4, formal

oxidation state of Sn. From the peak position, it is evident that Sn is in the form of SnO_2 in compound and no metallic Sn is detected.

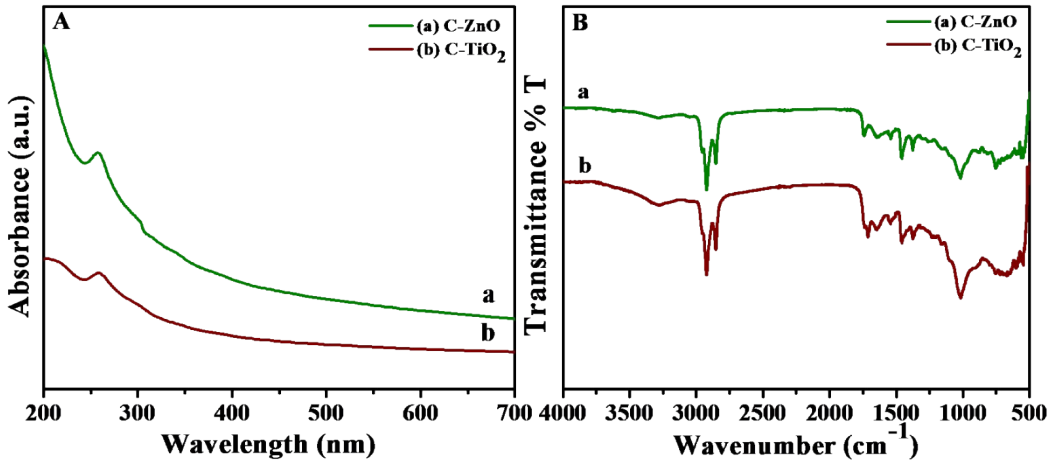

Figure S8 UV-Visible spectra (A), FTIR spectra (B) of C-ZnO (a) and C-TiO_2 (b) composite respectively.

The optical absorption spectra of C-ZnO and C-TiO_2 (**Figure S8** A) composite thin films on quartz plate shows clearly blue shifted absorption (lower wavelength) than that is reported for bulk materials respectively. This is attributed to smaller size of particles leading to quantum confinement effect in the film.[S2] The FTIR spectrum of C-ZnO (**Figure S8 B** (a)) shows the peak at 535 cm^{-1} ascribed to Zn-O stretching, suggesting formation of ZnO.[S3] The FTIR spectrum of C-TiO_2 composite shows a broad peak at 600 cm^{-1} which is ascribed to absorption bands of Ti–O and O–Ti–O,[S4] this confirms the formation of TiO_2. Moreover, for both composites, the presence of other peaks i.e. 2924, 2846, 1571, 1589, 1743 cm^{-1} are assigned to C-H stretching, C-C, C=C, C-OH or C-OO stretching respectively. These results are confirms the successive formation of the composite.

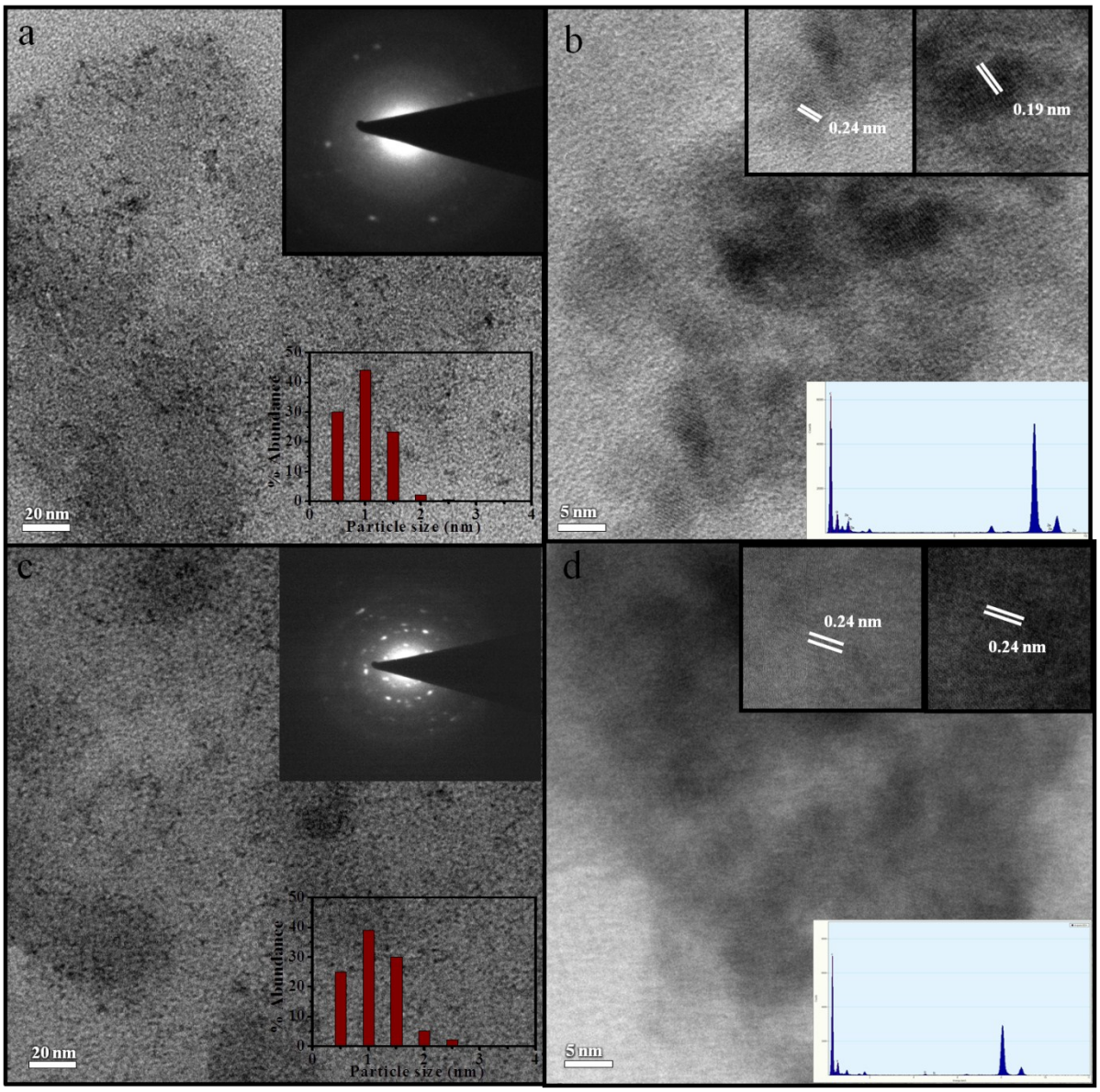

Figure S9 (a), (c) Low magnification TEM image of C-ZnO and C-TiO_2 composite, the insets shows selected area electron diffraction (SAED) (top) and particle size histogram (bottom) respectively. (b), (d) HRTEM image, an inset (top) shows enlarged image, and EDS spectra (bottom) of C-ZnO and C-TiO_2 composite respectively.

Figure S9 (a), (b), (c) and (d) are the TEM images of C-ZnO and C-TiO_2 composite. The low magnification image given in Figure S8 (a) and (c) clearly indicates un-agglomerated distinct particle**,** most of the particle lies below 2.5 nm (bottom inset of histogram (a and c). The formation of ZnO and TiO_2 is further confirmed by the selected area electron diffraction

(SAED) patterns for which the respective rings are indexed to hexagonal ZnO structure (JCPDS Card No. 79-205) and orthorhombic TiO_2 (JCPDS Card No. 82-1123). The HRTEM image of ZnO and TiO_2 QDs exhibits clear lattice fringes**,** with fringe spacing at 0.24 nm corresponds to sp^2 carbon and 0.19 nm, 0.24 nm, corresponding to the inter planar distance of (102) and (111) lattice planes of hexagonal ZnO and orthorhombic TiO_2, respectively.

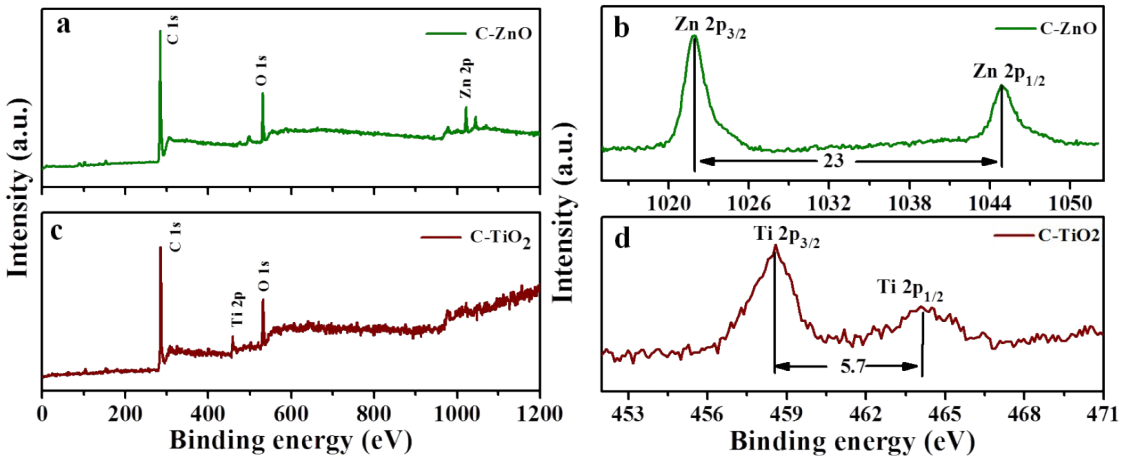

Figure S10 XPS spectra of (a), (c) general scan; (b), (d) Core level XPS spectra of Zn 2p and Ti 2p peaks of C-ZnO and C-TiO_2 composite respectively.

The general scans of the composite do not show other peaks than expected peaks. The Zn 2p spectrum of C-ZnO composite (b) shows a doublet feature arising due to spin-orbit splitting. The peak positions of Zn $2p_{3/2}$ and $2p_{1/2}$ are observed at 1021.7 and 1044.8 eV respectively, which is in agreement with spin orbit separation of 23.1 eV.[S5] While, two peaks at binding energies 458.5 and 464.2 eV with a separation by 5.7 eV are attributed to characteristic peaks of Ti $2p_{3/2}$ and Ti $2p_{1/2}$, respectively; indicating the presence of Ti^{4+} in TiO_2 in C-TiO_2 composite thin film.[S4]

Table S1. Quantitative measurement of elemental and chemical composition for C, SnO_2 and C-SnO_2 QDs composite by using XPS.

Compound	Elements	Chemical state	Binding Energy (eV)	% Composition
Carbon QDs	C 1s	C=C sp^2	284.1	19.33
		C-C sp^2	285.2	20.17
		C-O	286.4	7.46
		C=O	288.2	2.12
	O1s	O 1s	531.5	50.92
SnO_2 QDs	Sn 3d	Sn $3d_{5/2}$	486.5	78.95
		Sn $3d_{3/2}$	495	
	O 1s	O 1s	531.6	21.05
C-SnO_2 QDs (before charge/discharge cycles)	C 1s	M-C	281.9	2.65
		C=C sp^2	284	16.46
		C-C sp^2	285	19.77
		C-O	286.4	7.75
		C=O	288.2	1.82
	O1s	O 1s	531.5	28.36
	Sn 3d	Sn $3d_{5/2}$	486.5	23.19
		Sn $3d_{3/2}$	495	
C-SnO_2 QDs (after charge/discharge cycles)	C 1s	M-C	282.1	3.19
		C=C sp^2	283.67	15.5
		C-C sp^2	284.7	18.2
		C-O	286.5	3.09
		C=O	287.8	2.63
	O1s	O 1s	531.6	38.81
	Sn 3d	Sn $3d_{5/2}$	486.4	18.58
		Sn $3d_{3/2}$	494.9	

Table S2. Comparison of Specific capacitance Fg^{-1} obtained from Cyclic Voltammetry.

	Specific capacitance Fg^{-1} from Cyclic Voltammetry					**% Retention**
Scan rate	**20mVs^{-1}**	**50mVs^{-1}**	**100mVs^{-1}**	**150mVs^{-1}**	**200mVs^{-1}**	
SnO_2	220.3	201.3	185.1	167.3	159.2	71
Carbon	185.4	171.9	153.7	145.1	138.5	73
C-SnO_2	575.9	569.4	561.4	554.3	547.5	95

Table S3. Comparison of Specific capacitance Fg^{-1} obtained from galvanostatic charge discharge.

	Specific capacitance Fg^{-1} from Galvanostatic charge discharge					**% Retention**
Current density	**20mVs^{-1}**	**50mVs^{-1}**	**100mVs^{-1}**	**150mVs^{-1}**	**200mVs^{-1}**	
SnO_2	225.5	207.9	192.3	179.4	167.1	74.2
Carbon	190.2	184.5	162.1	141.2	140.5	73.9
C-SnO_2	578.5	573.1	564.8	559.9	552.8	96

References

[S1] S. Umrao, S. Abraham, F. Theil, S. Pandey, V. Ciobota, P. K. Shukla, C. J. Rupp, S. Chakraborty, R. Ahuja, J. Popp, B. Dietzek, A. Srivastava, *RSC Adv.*, 2014, **4**, 59890-59901.

[S2] L. E. Brus, *J. Chem. Phys.* 1984, **80**, 4403-4409.

[S3] S. H. Jung, E. Oh, K. H. Lee, Y. Yang, C. G. Park, W. Park, S. H. Jeong, *Cryst. Growth Des.* 2008**, 8**, 265-269.

[S4] L. Sikong, M. Masae, K. Kooptarnond, W. Taweepreda, F. Saito, *App. Sur. Sci.* 2012, **258**, 4436-4443.

[S5] A. H. Jadhav, S. H. Patil, S. D. Sathaye, K. R. Patil, *J. Mater. Sci.* 2014, **49**, 5945-5954.